ISSN 2075-1133, Inorganic Materials: Applied Research, 2021, Vol. 12, No. 2, pp. 262–270. © Pleiades Publishing, Ltd., 2021.
Russian Text © The Author(s), 2020, published in Perspektivnye Materialy, 2020, No. 10, pp. 5–18.

PHYSICOCHEMICAL FUNDAMENTALS OF CREATING MATERIALS AND TECHNOLOGIES

Influence of Ion Treatment Modes on the Physical and Mechanical Properties of Zirconia Ceramics

S. A. Ghyngazov[a], *, V. A. Kostenko[a], **, and A. K. Khassenov[b], ***

[a] *National Research Tomsk Polytechnic University, Tomsk, 634050 Russia*
[b] *Karaganda State University, Karaganda, 100026 Kazakhstan*
**e-mail: ghyngazov@tpu.ru*
***e-mail: kostenkova@tpu.ru*
****e-mail: ayanbergen@mail.ru*

Received April 6, 2020; revised June 22, 2020; accepted June 23, 2020

Abstract—The article considers the influence of the treatment modes with N^{2+} and Ar^{+} ions beams on the physical and mechanical properties of zirconia ceramics. Surface modification of zirconia ceramics was performed using two modes of ion treatment—pulsed and continuous. The pulsed mode of treatment with N^{2+} ions was realized at an accelerating voltage of 250–300 kV, current density j = 150–200 A/cm^2, and energy density W = (3.5 and 5) ± 5% J/cm^2. The continuous mode of treatment with Ar^{+} ions was realized at an accelerating voltage of 30 kV and an ion current density of 300 and 500 μA/cm^2. The fluence of the Ar^{+} ion beam varied from 10^{16} to 10^{18} cm^{-2}. It is established that the pulsed mode of ion treatment leads to the melting and recrystallization of the surface of ceramics. It is shown that this treatment leads to a violation of the oxygen stoichiometry in ceramics and, as a result, there is an appearance of electrical conductivity in the near-surface layers; the layers of zirconia ceramics become conductive. It is established that the continuous mode of ion treatment does not lead to the melting and recrystallization of the ceramic surface but is accompanied by its slight etching. It is shown that, under the action of continuous ion treatment, the microhardness increases (by 14%). Hardening of the surface layers of ceramics is observed at a depth that exceeds the average projected range of Ar^{+} ion by 10^3 times.

Keywords: zirconia ceramics, ion treatment, microhardness, electrical conductivity
DOI: 10.1134/S2075113321020179

INTRODUCTION

The treatment of materials by concentrated flows (CF) of accelerated particles is an efficient method of modification of their properties [1–5]. The treatment with electron [6–10] and ion [7, 11–15] concentrated flows is the most widely used. Such surface treatment allows controlled change in the functional properties of the materials if they directly depend on the state of the near-surface layers.

The progress in developments and modernization of accelerating techniques [12, 16] leads to the broadening of electron and ion beam parameters (accelerating voltage, ion current density, energy density), which are determinative at the modification of materials. Despite this fact, the question of choosing and justifying the irradiation regime (pulsed or continuous) remains relevant [17–21]. The impact efficiency and degree of structural-phase transformations in the near-surface layer depend on the choice of the irradiation mode for each material. The formation of specified mechanical, tribological, and electrical properties under the CF effect allows the widening of areas of their application [13–16]. Using the CF for the treatment of material and products makes it possible to significantly shorten the technological cycles and decrease the number of technological stages. All this opens up prospects for reducing energy consumption in the manufacture of products for a wide range of applications. Ion beams are widely used among the CF types. The efficiency of this treatment was proved on metals and alloys [16, 22–25]. In [26–29], the pulsed mode of treatment of the surface of metals and alloys with C^{+} and H^{+} ions was studied in detail. In particular, it was mentioned that, at an energy density of 1–5 J/cm^2 and current density of 150–200 A/cm^2, characteristic physical processes such as spraying, erosion, melting, and cracking of materials take place. As a result, the thickness of the modified layer is limited by the ratio of the physical processes listed above. It was noted that, despite the small thickness of the modified layer, there is simultaneous quenching and increasing mechanical and tribological properties of the prod-

ucts. Such effects of the pulsed ion treatment of metals and alloys are described in a number of works [14, 16, 30]. It was shown in [30, 31] that this method could be applied to clean turbine parts from soot and carbon deposits and strengthen cutting tools, extending their service life.

Processing of metals and alloys with a continuous ion beam is studied in [12, 23, 32, 33]. It is mentioned that there is surface spraying for such mode, but no fusing and cracking of surface layers are observed. According to [34], at irradiation of titanium target with Al^+ ions under accelerating voltage of 1.5 kV, current density about 200 mA/cm^2, and fluence of 1.3×20^{21} and 2.4×10^{21} cm^{-2} for 1 h, the thickness of the sprayed layer varies from 150 to 300 μm. As a result, after ion irradiation, the titanium target had the same elemental composition as before. It is noted in [23, 33] that, despite the absence of fusing and recrystallization at continuous irradiation with Ar^+ ions with a current density of 300–500 μA/cm^2 and accelerating voltage of 10–50 keV, there are structural-phase transformations and change in both mechanical and tribological properties of pure metals (Mo, Fe, Al) and $Fe_{65}Al_{35}$ and $Fe_{93.75}Si_{6.25}$ alloys.

The clarification of the ion modification mechanism is of great interest. A shock wave mechanism of the effect on metals and alloys was proposed for the continuous irradiation mode in [23, 32]. As a result, restructuring of the crystalline structure occurs, which leads to phase transitions and, consequently, change in the functional properties. It is noteworthy that such an effect takes place to a depth much greater than the ion path length. In [23], this phenomenon is called a "long-range effect" and it is used to explain the transformation of near-surface layers of the materials at a depth greater than the mean projected ion path length in a solid.

Analyzing the studies conducted on the modification of metals and alloys [12, 18, 19, 23, 31], it was concluded that the physical processes of erosion, fusing, and cracking typical of ion irradiation and, consequently, the physical transformation mechanism of the irradiated surface directly depend on the parameters of the ion beam and ion impact mode.

Besides products of metals and alloys, there is a growing interest in the industry in the application of ceramic construction materials. According to [7, 35, 36], the impact of CF of ions and electrons can be successfully used to modify ceramics and this method is promising for obtaining ceramic products with unique functional properties. Owing to the high chemical resistance, extremely high hardness, and high melting temperature of ceramics, there is no alternative to such treatment. In this regard, the choice of parameters and mode of individual ceramic materials is of great practical interest. Comparative analysis of pulsed and constant modes of such impact on ceramics has not been conducted yet; therefore, studies on the effect of characteristics and modes of radiation impact on ceramics are important for the development of technologies of their modification.

Zirconia ceramic is a widely used ceramic material [37, 38]. This ceramic is applied in the industry as an individual material and a part of composites. Introduced oxide additives can act as stabilizers improving the mechanical properties of the ceramic. Despite inherent polymorphism [44], zirconia ceramic is used in science and technology, including the automobile, aviation, and space industries [37]. Plain and rolling bearings, the lining of flow elements of chemical metering pumps, etc., are made of it. To improve mechanical resistance and stabilize the phase composition of zirconia ceramics, plasticizers, additives, and impurities are used in the production technology of details [45, 46]. Frequently, ceramic details are subjected to a mechanical treatment at the end of the technological cycle which can lead to destruction or cracking of the ceramic. This effect can be avoided using the ion treatment which can also be used for the creation of a surface conducting layer [42, 43] or surface hardening of ceramics [17, 36].

Owing to electrical insulating properties, zirconia ceramic is used to produce electrical insulating materials and parts for accelerator technology. Volume breakdown of the products can be prevented by the formation of a slightly conducting state on their surface which promotes charge draining. This reduces the risk of failure of electrical appliances and electrical installations. At present, multistage and energy-consuming techniques are used for the application of conducting coatings on ceramics [39–41]. As an alternative to these expensive methods, the surface treatment with CF of ions and electrons can be considered. It was shown in [42, 43] that, under the impact of accelerated particle CF, there is a disordering of the structure of ferrite lithium-titanium and zirconium ceramics leading to the disturbance of its stoichiometric composition by oxygen. As a result, the ceramic becomes conductive. The creation of a conducting ceramic surface by ion treatment without multistage spraying of metallic coating is under investigation [40, 41].

In practice, partly stabilized zirconia (PSZ) is widely used owing to its high stability at temperatures up to 2297°C [17, 47]. PSZ is applied as an industrial ceramic, thermal barrier coating, electroceramic, high-temperature magnetohydrodynamic electrodes, oxygen sensors, etc. This ceramic has high resistivity to radiation amorphization and it is structurally compatible with many radioactive oxides such as UO_2 and PuO_2, which makes possible its application in fuel elements. This variety of application areas is based on the combination of mechanical, electrical, thermal, and other properties of PSZ-based materials.

Depending on the ion beam parameters and ion irradiation mode, the crystalline structure and functional properties of the same ceramic material can be

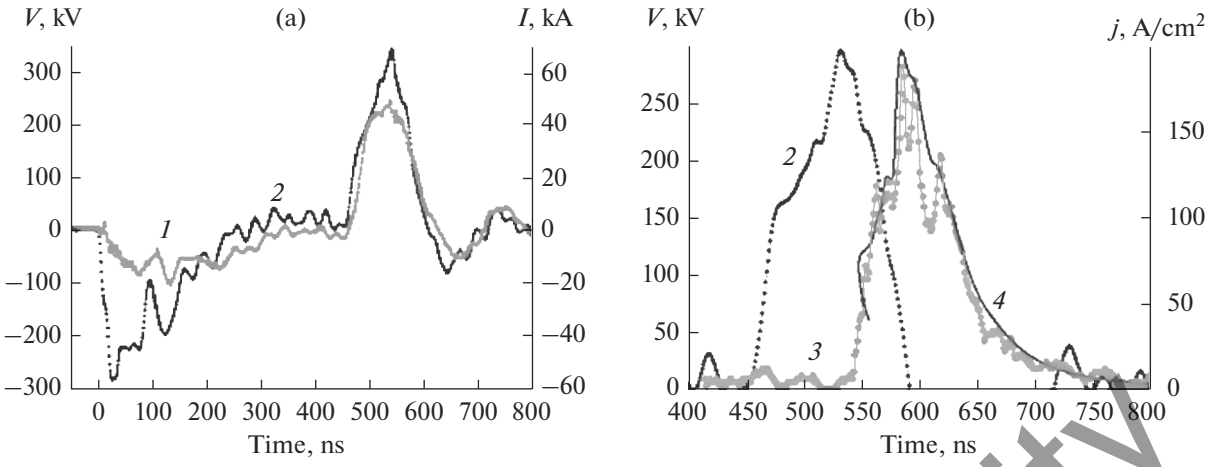

Fig. 1. Oscillograms of (*1*) the total current in a diode, (*2*) accelerating voltage, (*3*) ion current density, and (*4*) calculated N^{2+} ion density.

changed in different ways. The behavior of PSZ at different modes of ion irradiation has not been conducted yet. The search for optimal parameters and modes of ion modification of zirconia ceramics is a relevant task of modern materials sciences.

This work is aimed at the comparative analysis of the effect of PZS treatment with an intense pulsed beam of N^{2+} ions and a continuous beam of Ar^+ ions on change in its mechanical and electrophysical properties, including the depth of the near-surface layer subjected to the ion treatment. The choice of the mentioned treatment types is dictated by their wide application for the treatment and modification of metals and alloys.

EXPERIMENTAL

Ultrafine powder (UFP) of PSZ with composition ZrO_2–3 mol % Y_2O_3 was used as a starting material for preparation of the ceramic; the powder was obtained by decomposition of aqueous solutions of zirconium and yttrium nitrates in high-frequency discharge plasma [48]. It is known that UFPs obtained by this technology are characterized by the existence of hollow spheres and a high degree of agglomeration [48]. To reach a uniform particle size distribution, PSZ was treated in an Aktivator-2SL planetary mill for 30 min. The ratio of ball weight to the powder weight was 1.5; the drum rotation speed was 1500 rpm.

Pressing of UFP to pellets with a diameter of 9 mm and a thickness of 2.9–3.2 mm was conducted by cold static uniaxial pressing in a closed mold. The pressing pressure was about 150 MPa. To reduce the wall friction between the walls of the mold and the punch, graphite lubricant was used. The pressed samples were sintered in a SNOL 12/16 high-temperature muffle furnace at a temperature of 1673 K for one hour.

The density and open porosity of the sintered ceramic was determined by hydrostatic weighing in distilled water. The average density of the sintered ceramic ρ was 5.8 g/cm^3, and the open porosity was less than 5%. X-ray diffraction analysis of the ceramic was performed using an ARL X'TRA diffractometer with monochromic CuK_α radiation in a 2θ range of 10°–90°. The XRD patterns were processed by full-profile analysis using PowderCell 2.4 software.

The microhardness H_V was determined by a restored print using a Vickers four-sided diamond pyramid at a load P of 3 N on the indenter. The average value of ceramic microhardness H_V was calculated by a set of statistical data. The uncertainty of H_V measurement was determined as the standard deviation. Before microhardness measurements, one side of the zirconia ceramic samples was mechanically treated using an Al_2O_3 abrasive powder with a particle size of 20 and 3–5 μm. According to [49], this treatment method caused $t \rightarrow m$ phase transformation to a depth of several microns in the near-surface layer. To eliminate the induced m phase, the sample surface was polished by a diamond paste with a particle size of 0.5–1 μm. After the mechanical treatment, the ceramic grain structure vanishes, but pores and scratches from the abrasive treatment are clearly seen on the surface.

Surface treatment of the ceramic under the pulsed and continuous modes of ion processing was conducted on the polished side. The pulsed mode was implemented for N^{2+} ions on a TEMP-6 accelerator [50]. The ion beam parameters were the following: accelerating voltage E = 250–300 kV, current density j = 150–200 A/cm^2, and energy density W = (3.5 and 5) ± 5% J/cm^2. The number of pulses N was 2. Typical diode assembly oscillograms are given in Fig. 1. The density of N^{2+} ions (Fig. 1, curve *4*) was calculated by the technique described in [51].

Table 1. Beam parameters under treatment of zirconia ceramics with Ar^+ ions

Mode	Accelerating voltage, U, keV	Current density, j, μA/cm^2	Sample number, i	Fluence, $F \times 10^{16}$, cm^{-2}
A_i	30	300	1	0.94
			2	2.4
			3	9
			4	11
			5	50
			6	100
B_i		500	1	2.2
			2	12
			3	100

The continuous mode was implemented for the treatment with Ar^+ ions using a PULSAR ion implanter [52] with a source of ions with average energy. The ceramic was treated at an accelerating voltage of 30 kV and ion current density j of 300 and 500 μA/cm^2. The beam fluence was varied from 10^{16} to 10^{18} cm^{-2}. Table 1 lists all modes of the ion treatment of ceramic samples using the PULSAR implanter.

The microstructure of ceramic samples before and after ion treatment was studied by scanning electron microscopy (SEM) using a Hitachi TM-3000 microscope equipped with a backscattered electron detector. To remove the charge from the ceramic, its surface was covered with a thin conducting metallic layer with a thickness of no more than 100 nm.

The conductivity was measured by the two-probe method in a temperature range of $T = 298–573$ K [53]. Constant voltage $U_{max} = 5$ V was applied to the electrodes during measurements. Activation energy E_a of volume conductivity at the certain depth of the modified ceramic was determined by the results of treatment of the conductivity temperature dependence.

Change in H_V and E_a in the ceramic versus depth was determined at subsequent removal of thin modified layers. The layers were removed by mechanical polishing using an Al_2O_3 abrasive with a particle size of 0.5–1 μm. The thickness of the removed layer was determined using an I4 dial indicator (GOST 577-68) by measuring the residual thickness of the ceramic. The micrometer resolution (scale division) is 10 μm.

RESULTS AND DISCUSSION

Samples in the initial state after sintering were white in color as is typical of zirconia ceramics. The grain structure was determined on their surface; the grain size changed from 0.5 to 1 μm.

It was established that the pulsed treatment with N^{2+} ions at $j = 150–200$ A/cm^2 and $W = 3.5$ and 5 J/cm^2, as well as the impact with continuous Ar^+ ion beam in the A and B modes with $f = 10^{16}–10^{18}$, leads to blackening of ceramic samples. At the pulsed treatment with N^{2+} ions, the blackening occurs not only on the side of ion beam impact but also through the ceramic volume. At the same time, blackening is observed only on the side under the ion beam effect at the treatment with the continuous Ar^+ ion beam. This difference can be explained by different heating of the ceramic volume depending on the ion treatment mode.

Figure 2 presents SEM images of the ceramic surface before and after the treatment with N^{2+} and Ar^+ ions. In the initial state (before ion treatment), the ceramic surface after polishing is fairly smooth (Fig. 2a). Randomly distributed pores and defects can be observed on the surface.

The treatment with N^{2+} pulsed ion beams (PIB) leads to fusing followed by crystallization and formation of cracks and small craters over the surface of ceramic samples (Figs. 2b and 2c). As follows from the analysis of the sample surface after pulsed ion treatment with the energy density of 3.5 and 5 J/cm^2, the character of crystallization of fused surface is similar. The largest amount of craters is observed in the location of pores and defects.

It was established that the effect of the Ar^+ continuous ion beam (CIB) does not cause the formation of cracks, fusing, and recrystallization of the ceramic surface. Such type of ion treatment leads to the visualization of the grain structure of the ceramic (Fig. 2d). The CIB treatment in mode A leads to uneven visualization of grains over the ceramic surface. First of all, the clear appearance of grains is observed in the locations of pores and defects. Treatment in mode B leads to an even grain visualization over the ceramic surface owing to a difference in the rates of ion leaching of grain volume and grain boundaries. The leaching rate in grain boundaries is significantly higher because of the largest defectiveness.

Thus, the change in microrelief of ceramic samples depends on the mode of ion treatment and ion beam parameters.

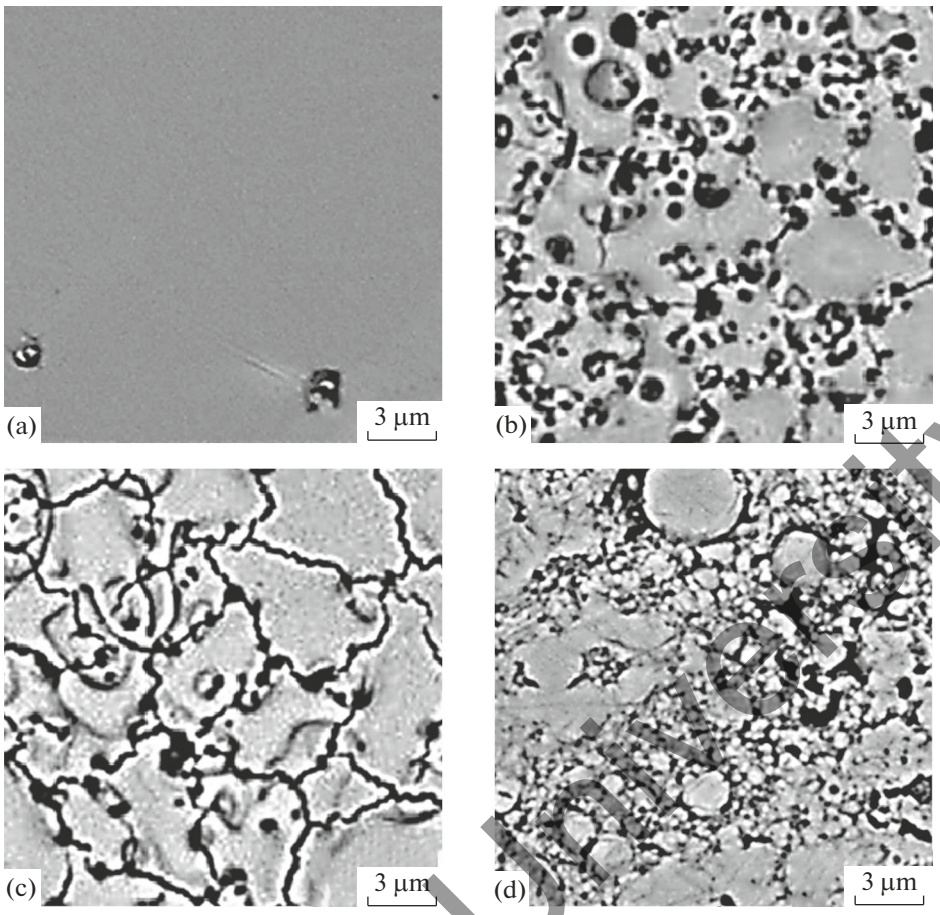

Fig. 2. SEM images of surface of zirconia ceramics: (a) initial polished surface; (b, c) after treatment in pulsed mode with N^{2+} ions with $W = 3.5$ J/cm^2 (b) and $W = 5$ J/cm^2 (c), respectively; (d) after treatment in constant mode with Ar^+ ions with $f = 10 \times 16$ cm^{-2}.

Electrical Conductivity of Zirconia Ceramics

The electrical conductivity of ceramic samples was measured before and after the ion effect. At conductivity measurements of unirradiated ceramic samples within the limits of sensitivity of the equipment used (1 nA), no current was fixed through measuring probes.

The treatment with Ar^+ CIB does not cause the appearance of conductivity of near-surface layers of the ceramic within the limits of sensitivity of the measuring device. Consequently, despite the change in color of the treated surface, no significant oxygen nonstoichiometry leading to noticeable conductivity growth occurs.

The N^{2+} PIB effect on ceramic samples leads to increase in the electrical conductivity of their near-surface layers. In [42, 43], such behavior is connected with violation of the stoichiometry of the ceramic surface due to presumable oxygen desorption under ion treatment.

The temperature dependences of conductivity of the ceramic modified under the impact of N^{2+} PIB are given in Fig. 3. As is seen (Fig. 3, curve *1*), at the first measurement, the conductivity is fixed in a range from 312 to 405 K. At the repeated measurement, the conductivity decreases significantly (Fig. 3, curve *2*), which indicates intense oxidation processes during measurements of conductivity. These processes spread to the full depth of the modified layer. This fact is evidenced by the changing character of conductivity after layer-by-layer removal of thin layers (Fig. 3, curves *3* and *4*).

Thus, upper layers of the ceramic surface transformed from the conducting state to the state of decreased conductivity during heating at the time of measurements.

The transition of surface ceramic layers in the condition with increased conductivity is accompanied by decrease in the activation energy E_a from 9.3 to 1.36 eV. The values of E_a over the depth of the sample treated are given in Table 2. It is seen that, at the first measurements (Fig. 3, curve *1*), the conductivity values were 8.8×10^{-5} and 1.8×10^{-4} $(\Omega\ \text{cm})^{-1}$ at the temperatures of 323 and 405 K, respectively. At the fourth

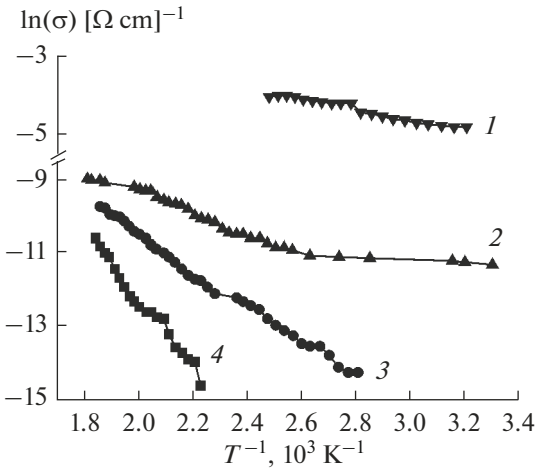

Fig. 3. Temperature dependence of electrical conductivity of zirconia ceramics after pulsed ion treatment at $W = 5$ J/cm^2: (*1*) the first measurement; (*2*) the second measurement; (*3*, *4*) the measurement after removing the modified layer.

measurement, the conductivity decreased significantly, and it was possible to measure only in a temperature range from 450 to 550 K (Fig. 3, curve *4*). The conductivity value at the fourth measurement was 5.3×10^{-9} and 2.12×10^{-7} $(\Omega\ \text{cm})^{-1}$ at 450 and 550 K, respectively. Activation energy E_a was determined by approximation of curves given in Fig. 3 by a linear dependence; E_a values were 1.36 and 9.3 eV for the first and the fourth measurements. The activation energy grows as the number of measurements accompanied by heating to 573 K increases, which is typical of oxidation processes.

Thus, it is shown that the removal of oxidized modified layers, in general, does not lead to increasing conductivity and decreasing activation energy of ceramics to the value obtained at the first measurement. It indicates that the modified ceramic layers oxidize, and the oxygen stoichiometric composition is restored, which leads to reduction in the conductivity and growth in E_a.

Microhardness of Zirconia Ceramics

The microhardness H_V of ceramic samples was measured before and after ion treatment at the loading on indenter of 3 N. Under such load, the depth of indentation in the zirconia ceramic is $h_v = 3 \pm 0.06$ μm. The H_V of zirconia ceramic before ionic treatment was 11 ± 0.5 GPa.

After the impact of N^{2+} PIB, the microhardness cannot be measured by the recovered fingerprint method because of a strong fusing of the surface and formation of craters. The microhardness was determined only after layer-by-layer removal of layers at conductivity measurements. The H_V value was 10 ± 1 GPa. Similar H_V values before and after N^{2+} PIB demonstrate that all of the modified layer was removed during conductivity measurements.

Depth measurement of H_V after the treatment with Ar^+ CIB was performed for ceramic samples with the highest increase in H_V of the modified near-surface layer. After the treatment of the ceramic with Ar^+ CIB in mode A with $f = 1.1 \times 10^{17}$ cm^{-2}, H_V increased from 11 ± 0.5 to 13.1 ± 0.2 GPa. After the treatment in mode B at fluences of 2.2×10^{16} and 10^{18} cm^{-2}, the H_V values were 12.1 ± 0.2 and 12.3 ± 0.2 GPa, respectively; i.e., the H_V gain for these fluences was almost equal. Figure 4 demonstrates the plot of change in H_V over depth depending on the mode and parameters of ion treatment. The sample surface after ion treatment was taken as a zero point of reference. As is seen from Fig. 4, the H_V value shifts toward the value before the ion treatment as each thin modified layer is removed. The thickness of the removed modified layer of the ceramic is about 20 μm.

As mentioned above, Ar^+ CIB treatment does not cause the fusing of the sample surface layer. The spraying of the surface after treatment in mode B is higher

Table 2. Electrical conductivity and activation energy of zirconia ceramics after pulsed ion treatment

Curve number (Fig. 3)	Measurement temperature, T, K	Conductivity, σ, $(\Omega\ \text{cm})^{-1}$	Activation energy, E_a, eV
1	323	8.8×10^{-5}	1.36
	405	1.8×10^{-4}	
2	320	1.5×10^{-7}	1.84
	573	1.3×10^{-6}	
3	350	3.1×10^{-9}	4.7
	540	6.2×10^{-7}	
4	450	5.3×10^{-9}	9.3
	550	2.1×10^{-7}	

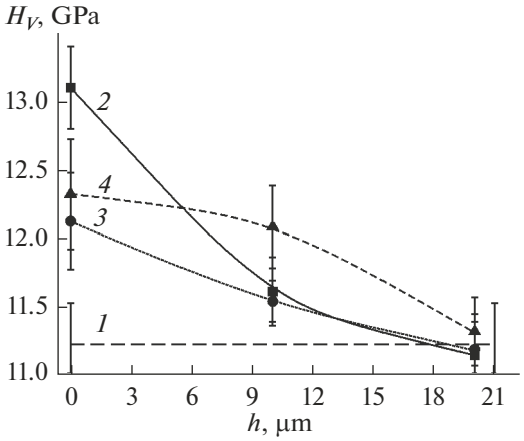

Fig. 4. Microhardness H_V of ceramics versus thickness before (*1*) and after (*2–4*) treatment with Ar^+ ions: (*2*) j = 300 μA/cm^2, $f = 1.1 \times 10^{17}$ cm^{-2}; (*3*, *4*) j = 500 μA/cm^2, $f = 2.2 \times 10^{16}$ and 10^{18} cm^{-2}, respectively

than in mode A. This can explain a higher H_V value after the ion treatment in mode A compared with mode B. The observed change in H_V of the ceramic takes place at the depth of more than 20 μm. According to [17], the projective path of Ar^+ ions in zirconia ceramics is ~20 nm. Therefore, we guess that the shock wave mechanism of ceramic hardening at the depth exceeding the projective path of Ar^+ ions can be proposed by analogy to the processing of metals and alloys. This mechanism is realized as the propagation of post-cascade elastic and shock waves and generation of defects, including dislocations in places of static stresses, which increase with the irradiation dose of the implanted ions, and the propagation of these dislocations deep into the substance [23]. Post-cascade elastic and shock waves lead to the broadening of the zone of ion effect in the material to several tens of microns and more. Thus, the ion treatment sharply increases the mobility of atoms (both intermediate and substitute) initiating crystalline restructuring in metastable media, thereby changing the strength properties of the material.

The thickness of the modified ceramic layer under the effect of N^{2+} PIB is about 30 μm, while after the treatment with the continuous Ar^+ beam this value is ~20 μm. The difference in the modified ceramic layer is connected with different treatment modes. Heat and shock-wave beam impact is essential for the degree of ceramic modification with N^{2+} PIB, and it causes not only disturbance of the crystalline structure of ceramics but recrystallization of surface layers. In the CIB mode, there is only the shock-wave effect on the ceramics, which is not accompanied by the following surface recrystallization but affects the crystal structure of zirconia ceramics.

CONCLUSIONS

The effect of pulsed and continuous modes of ion treatment on the mechanical and electrophysical properties of zirconia ceramics was considered.

The pulsed mode of N^{2+} ion treatment at the current density j of 150–200 A/cm^3 and energy density W of (3.5 and 5) ± 5% J/cm^2 leads to fusing and recrystallization of the ceramic surface. Such type of surface treatment causes disturbance of the oxygen stoichiometric composition, which leads to the appearance of conductivity in near-surface layers.

Continuous treatment with Ar^+ ions at the current densities j of 300 and 500 μA/cm^2 with the fluence from 10^{16} to 10^{18} cm^{-2} does not cause fusing and recrystallization of the ceramic surface but leads to its spraying. Such surface treatment increases the microhardness (by 14%). The hardening of modified ceramic layers is observed at a depth that exceeds the average projected ion path by 10^3 times.

It was shown that, under the ion treatment, one can reach both a structural change and conducting state of the surface, as well as increase in the microhardness of the surface layers of zirconia ceramics. The degree and character of ceramic modification is determined by the modes and parameters of ion treatment.

FUNDING

This work was supported by the Ministry of Science and Higher Education of the Russian Federation within the scope of the Nauka program (project no. FSWW-2020-0008) and competitiveness improvement programs of Tomsk Polytechnic University.

REFERENCES

1. Chernov, V.M., Radiation properties of the metal structural materials during low-temperature damaging irradiation, *Perspekt. Mater.*, 2018, no. 5, pp. 23–40.
2. Gribkov, V.A., Demin, A.S., Demina, E.L., Epifanov, N.A., Latyshev, S.V., Lyakhovitsky, M.M., Maslyayev, S.A., Morozov, E.V., Pimenov, V.N., Sasinovskaya, I.P., Sirotinkin, V.P., Sprygin, G.S., and Timoshina, M.I., Specifics of damageability of the silicon single crystal under exposure of powerful plasma streams and fast helium ions, *Inorg. Mater.: Appl. Res.*, 2020, vol. 11, pp. 349–358. https://doi.org/10.1134/S2075113320020136
3. Karsch, L., Beyreuther, E., Enghardt, W., Gotz, M., Masood, U., Schramm, U., Zeil, K., and Pawelke, J., Towards ion beam therapy based on laser plasma accelerators, *Acta Oncol.*, 2017, vol. 56, no. 11, pp. 1359–1366.
4. Yastrebinskii, R.N., Bondarenko, G.G., and Pavlenko, V.I., Radiation hardening of constructional cement–magnetite–serpentinite composite under gamma irradiation at increased dose, *Inorg. Mater.: Appl. Res.*, 2017, vol. 8, no. 5, pp. 691–695.

5. Demina, E.V., Gribkov, V.A., Prusakova, M.D., Pimenov, V.N., Morozov, E.V., Maslyaev, S.A., Voronin, A.V., Gusev, V.K., Garkusha, I.E., Makhlai, V.A., Laas, T., Shirokova, V., and Vali, B., Surface structure transformation in double forged tungsten upon single and sequenced irradiation using different types of radiation facilities, *Inorg. Mater.: Appl. Res.*, 2018, vol. 9, pp. 832–847. https://doi.org/10.1134/S2075113318050088
6. Gromov, V.E., Gorbunov, S.V., Ivanov, Y.F., Vorobiev, S.V., and Konovalov, S.V., Formation of surface gradient structural-phase states under electronbeam treatment of stainless steel, *J. Surf. Invest.: X-ray, Synchrotron Neutron Tech.*, 2011, vol. 5, pp. 974–978.
7. Ghyngazov, S.A., Zirconia ceramics processing by intense electron and ion beams, *Nucl. Instrum. Methods Phys. Res., Sect. B,* 2018, vol. 435, pp. 190–193.
8. Ivanov, Yu.F., Koval, N.N., Gorbunov, S.V., Vorobyov, S.V., Konovalov, S.V., and Gromov, V.E., Multicyclic fatigue of stainless steel treated by a high-intensity electron beam: Surface layer structure, *Russ. Phys. J.*, 2011, vol. 54, pp. 575–583.
9. Zehra Nur Ozer, Electron beam irradiation processing for industrial and medical applications, *EPJ Web Conf.*, 2017, vol. 154, art. ID 01019.
10. Ivanov, Y.F., Alsaraeva, K.V., Gromov, V.E., Popova, N.A., and Konovalov, S.V., Fatigue life of silumin treated with a high-intensity pulsed electron beam, *J. Surf. Invest.: X-ray, Synchrotron Neutron Tech.*, 2015, vol. 9, no. 5, pp. 1056–1059.
11. Yea, C., Xue, J., Liu, T., Shu, R., Yan, Y., Liao, Y., Ren, Q., Rana, G., Sun, K., Jiang, L., Xiu, P., and Wangce, L., The microstructure evolution in a SiC_f/SiC composite under triple ion beam irradiation, *Ceram. Int.*, 2020, vol. 46, no. 7, pp. 9901–9906.
12. Ryabchikov, A.I., Progress in low energy high intensity ion implantation method development, *Surf. Coat. Technol.*, 2020, vol. 388, art. ID 125561.
13. Demin, A.S., Morozov, E.V., Maslyaev, S.A., Pimenov, V.N., Gribkov, V.A., Demina, E.V., Sasinovskaya, I.P., Sirotinkin, V.P., Sprygin, U.S., Bondarenko, G.G., Tikhonov, A.N., and Gaidar, A.I., The influence of a powerful stream of deuterium ions and deuterium plasma on the structural state of the surface layer of titanium, *Inorg. Mater.: Appl. Res.*, 2017, no. 3, pp. 412–418.
14. Zatsepin, D.A., Cholakh, S.O., and Vainshtein, I.A., *Ionnaya modifikatsiya funktsional'nykh materialov* (Ion Modification of Functional Materials), Ekaterinburg: Ural. Fed. Univ., 2014.
15. Elke, W. and Werner, W., *Ion Beam Modification of Solids*, New York: Springer, 2016.
16. Was, G.S, *Fundamentals of Radiation Materials Science: Metals and Alloys*, Springer, 2016.
17. Ghyngazov, S., Ovchinnikov, V., Kostenko, V., Gushchina, N., and Makhinko, F., Surface modification of $ZrO_2–3Y_2O_3$ ceramics with continuous Ar^+ ion beams, *Surf. Coat. Technol.*, 2020, vol. 388, art. ID 125598.
18. Konusov, F., Pavlov, S., Lauk, A., Tarbokov, V., Karpov, S., Karpov, V., Gadirov, R., Kashkarov, E., and Remnev, G., Effect of short-pulsed 200 keV C^+ ion beam and continuous 350 keV He^{2+} ion beam irradiation on optical properties of Al–Si–N coatings with a various Si content, *Surf. Coat. Technol.*, 2020, vol. 389, art. ID 125564.
19. Bedin, S.A., Ovchinnikov, V.V., Remnev, G.E., et al., Radiation stability of metal $Fe_{0.56}Ni_{0.44}$ nanowires exposed to powerful pulsed ion beams, *Phys. Met. Metallogr.*, 2018, vol. 119, pp. 44–51.
20. Bayu Aji, L.B., Wallace, J.B., and Kucheyev, S.O., Radiation defect dynamics in 3C-, 4H-, and 6H-SiC studied by pulsed ion beams, *Nucl. Instrum. Methods Phys. Res., Sect. B*, 2018, vol. 435, pp. 8–11.
21. Ghyngazov, S., Kostenko, V., Shevelev, S., Lysenko, E., and Surzhikov, A., Ion modification of alumina ceramics, *Nucl. Instrum. Methods Phys. Res., Sect. B*, 2020, vol. 464, pp. 89–94.
22. Mei, X., Zhang, X., Liu, X., and Wang, Y., Effect on structure and mechanical property of tungsten irradiated by high intensity pulsed ion beam, *Nucl. Instrum. Methods Phys. Res., Sect. B*, 2017, vol. 406, pp. 697–702.
23. Ovchinnikov, V.V., Nanoscale dynamic and long-range effects under cascade-forming irradiation, *Surf. Coat. Technol.*, 2018, vol. 355, pp. 65–83.
24. Zhu, H., Ma, Y., Wei, T., Li, H.J., Aughterson, R., and Lumpkin, G., The formation and Kr-ion irradiation behaviour of new microstructural features in additively manufactured titanium aluminium alloy, *Add. Manuf.*, 2019, vol. 29, art. ID 100766.
25. Jin, K., Velisa, G., Xue, H., Yang, T., Bei, H., Weber, W.J., Wang, L., and Zhang, Y., Channeling analysis in studying ion irradiation damage in materials containing various types of defects, *J. Nucl. Mater.*, 2019, vol. 517, pp. 9–16.
26. Slobodyan, M.S., Pavlov, S.K., and Remnev, G.E., Corrosion and high-temperature steam oxidation of E110 alloy and its laser welds after ion irradiation, *Corros. Sci.*, 2019, vol. 152, pp. 60–74.
27. Zou, H., Zhang, L., Guan, T., Zhang, X., Remnev, G.E., Pavlov, S.K., Wang, Y., and Mei, X., Effect on mechanics properties and microstructure of molybdenum by high intensity pulsed ion beam irradiation, *Surf. Coat. Technol.*, 2020, vol. 384, art. ID 125333.
28. Yu, X., Zhong, H., Zhang, Z., Shen, J., Zhang, J., Cui, X., Liang, G., Zhang, X., Zhang, G., Yan S., Wen, P., and Le, X., Hydrodynamic effects on the surface morphology evolution of aluminum alloy under intense pulsed ion beam irradiation, *Nucl. Instrum. Methods Phys. Res., Sect. B,* 2017, vol. 409, pp. 158–162.
29. Zhang, J., Yu, X., Zhong, H., Wei, B., Qu, M., Shen, J., Zhang, Y., Yan, S., Zhang, G., Zhang, X., and Le, X., The ablation mass of metals by intense pulsed ion beam irradiation, *Nucl. Instrum. Methods Phys. Res., Sect. B*, 2015, vol. 365, pp. 210–213.
30. Borovitskaya, I.V., Gribkov, V.A., Grigorovich, K.V., Demin, A.S., Maslyaev, S.A., Morozov, E.V., Pimenov, V.N., Sprygin, G.S., Zepelev, A.B., Gusakov, M.S., Logachev, I.A., Bondarenko, G.G., and Gaidar, A.I., Effect of pulsed helium ion fluxes and helium plasma on the inconel 718 alloy, *Russ. Metall. (Metally)*, 2018, vol. 2018, pp. 826–834.
31. Remnev, G.E., Isakov, I.F., Pushkarev, A.I., et al., High intensity pulsed ion beam sources and their indus-

trial applications, *Surf. Coat. Technol.*, 1999, vol. 114, pp. 206–212.

32. Romanov, Yu.I., Gushchina, N.V., Ovchinnikov, V.V., Makhinko, F.F., Stepanov, A.V., Medvedev, A.I., Starodubtsev, Yu.N., Belozerov, V.Ya., and Loginov, B.A., The effect of ion irradiation on nanocrystallization and surface relief of a ribbon from $Fe_{72.5}Cu_1Nb_2Mo_{1.5}Si_{14}B_9$, *Russ. Phys. J.*, 2018, vol. 60, pp. 1823–1831.
33. Ovchinnikov, V.V., Gushchina, N.V., Gapontseva, T.M., Chashchukhina, T.I., Voronova, L.M., Pilyugin, V.P., and Degtyarev, M.V., Optimal deformation and ion irradiation modes for production of a uniform submicrograin structure in molybdenum, *High Pressure Res.*, 2015, vol. 35, no. 3, pp. 300–309.
34. Ryabchikov, A., Shevelev, A., Sivin, D., Kashkarov, E., Bozhko, I., and Stepanov, I., High intensity low aluminum ion energy implantation into titanium, *Proc. 22nd Int. Conf. on Ion Implantation Technology, September 16–21, 2018, Würzburg, Germany,* pp. 364–367.
35. Maslyaev, S.A., Morozov, E.V., Romakhin, P.A., Pimenov, V.N., Gribkov, V.A., Tikhonov, A.N., Bondarenko, G.G., Dubrovsky, A.V., Kazilin, E.E., Sasinovskaya, I.P., and Sinitsyna, O.V., Damage of Al_2O_3 ceramics under the action of pulsed ion and plasma fluxes and laser irradiation, *Inorg. Mater.: Appl. Res.*, 2016, no. 3, pp. 330–339.
36. Ghyngazov, S., Pavlov, S., Kostenko, V., and Surzhikov, A., Ion processing of alumina ceramics by high-power pulsed beam, *Nucl. Instrum. Methods Phys. Res., Sect. B*, 2018, vol. 120, pp. 120–123.
37. Ajay Kumar Mishra, *Smart Ceramics: Preparation, Properties, and Applications*, Stanford, 2018.
38. Emelyanov, A.V., Nikiruy, K.E., Demin, V.A., Rylkov, V.V., Belov, A.I., Korolev, D.S., Gryaznov, E.G., Pavlov, D.A., Gorshkov, O.N., Mikhaylov, A.N., and Dimitrakis, P., Yttriastabilized zirconia cross-point memristive devices for neuromorphic applications, *Microelectron. Eng.*, 2019, vol. 215, art. ID 110988.
39. Chmielewski, T. and Golański, D., Selected properties of Ti coatings deposited on ceramic AlN substrates by thermal spraying, *Weld. Int.*, 2013, vol. 27, no. 8, pp. 604–609.
40. Komarov, S.V. and Romankov, S.E., Mechanical metallization of alumina substrate through shot impact treatment, *J. Eur. Ceram. Soc.*, 2014, vol. 34, no. 2, pp. 391–399.
41. Goreev, A.K., Burdovitsin, V.A., Klimov, A.S., and Oks, E.M., Electron-beam welding of ceramics with metal by using fore-vacuum plasma electron source, *Inorg. Mater.: Appl. Res.*, 2012, vol. 3, pp. 446–449.
42. Gyngazov, S.A., Ryabchikov, A.I., Kostenko, V., and Sivin, D.O., Aluminum ion beam treatment of zirconium ceramics, *Russ. Phys. J.*, 2018, vol. 61, pp. 1513–1519.
43. Frangulyan, T.S. and Ghyngazov, S.A., Ion treatment effect on the electrical conductivity of the surface layers of polycrystalline oxide semiconductors, *Sistemy. Metody. Tekhnol.*, 2014, no. 1(21), pp. 107–111.
44. Sathyaseelan, B., Manikandan, E., Baskaran, I., Senthilnathan, K., Sivakumar, K., Moodley, M.K., Ladchumananandasivam, R., and Maaza, M., Studies on structural and optical properties of ZrO_2 nanopowder for opto-electronic applications, *J. Alloys Compd.*, 2017, vol. 694, pp. 556–559.
45. Binner, J., Bala, V., Anish, P., Ketharam, A., and Bala, R., Compositional effects in nanostructured yttria partially stabilized zirconia, *Int. J. Appl. Ceram. Technol.*, 2011, no. 8, pp. 766–782.
46. Surzhikov, A.P., Ghyngazov, S.A., Frangulyan, T.S., Vasil'ev, I.P., and Chernyavskii, A.V., Investigation of sintering behavior of ZrO_2 (Y) ceramic green body by means of nonisothermal dilatometry and thermokinetic analysis, *J. Therm. Anal. Calorim.*, 2017, vol. 128, pp. 787–794.
47. Limarga, A.M., Iveland, J., Gentleman, M., Lipkin, D.M., and Clarke, D.R., The use of Larson–Miller parameters to monitor the evolution of Raman lines of tetragonal zirconia with high temperature aging, *Acta Mater.*, 2011, vol. 59, no. 3, pp. 1162–1167.
48. Larin, V.C., Kondakov, V.M., Maliy, E.N., Matyukha, V.A., Dedov, N.V., Kutyavin, E.M., Sennikov, Yu.N., Stepanov, I.A., and Ivanov, Yu.F., Plasmochemical method for obtaining nano-metal oxide powders and perspective directions of their application, *Izv. Vyssh. Uchebn. Zaved., Tsvetn. Metall.*, 2003, no. 5, pp. 59–64.
49. Frangulyan, T.S., Vasil'ev, I.P., and Ghyngazov, S.A., Effect of grinding and subsequent thermal annealing on phase composition of subsurface layers of zirconia ceramics, *Ceram. Int.*, 2018, vol. 44, pp. 2501–2503.
50. Zhu, X.P., Lei, M.K., and Ma, T.C., Characterization of a high-intensity bipolar-mode pulsed ion source for surface modification of materials, *Rev. Sci. Instrum.*, 2002, vol. 73, pp. 1728–1733.
51. Pushkarev, A.I., Egorova, Y.I., Prima, A.I., Korusenko, P.M., and Nesov, S.N., *Generatsiya, diagnostika i primenenie moshchnykh ionnykh puchkov s vysokoi plotnost'yu energii* (Generation, Diagnostics and Application of Powerful Ion Beams with High Energy Density), Novosibirsk: ANS SibAK, 2019.
52. Gavrilov, N.V., Mesyats, G.A., Nikulin, S.P., Radkovskii, G.V., Eklind, A., Perry, A.J., and Treglio, J.R., A new broad beam gas ion source for industrial applications, *J. Vac. Sci. Technol.*, 1996, no. 14, pp. 1050–1055.
53. Miroshkin, V.P., Panova, Ya.I., and Pasynkov, V.V., Dielectric relaxation in polycrystalline ferrites, *Phys. Status Solidi A*, 1981, vol. 66, no. 2, pp. 779–782.

Translated by N. Saetova